



HAL
open science

Provenance study of oyster shells by LA-ICP-MS

Vincent Mouchi, Camille Godbillot, Catherine Dupont, Marc-Antoine Vella, Vianney Forest, Alexey Ulianov, Franck Lartaud, Marc de Rafélis, Laurent Emmanuel, Eric P. Verrecchia

► To cite this version:

Vincent Mouchi, Camille Godbillot, Catherine Dupont, Marc-Antoine Vella, Vianney Forest, et al.. Provenance study of oyster shells by LA-ICP-MS. *Journal of Archaeological Science*, 2021, 132, pp.105418. 10.1016/j.jas.2021.105418 . hal-03284352

HAL Id: hal-03284352

<https://hal.science/hal-03284352v1>

Submitted on 8 Sep 2021

HAL is a multi-disciplinary open access archive for the deposit and dissemination of scientific research documents, whether they are published or not. The documents may come from teaching and research institutions in France or abroad, or from public or private research centers.

L'archive ouverte pluridisciplinaire **HAL**, est destinée au dépôt et à la diffusion de documents scientifiques de niveau recherche, publiés ou non, émanant des établissements d'enseignement et de recherche français ou étrangers, des laboratoires publics ou privés.

Provenance study of oyster shells by LA-ICP-MS

Vincent Mouchi^{1*}, Camille Godbillot¹, Catherine Dupont², Marc-Antoine Vella³, Vianney Forest⁴, Alexey Ulianov⁵, Franck Lartaud⁶, Marc de Rafélis⁷, Laurent Emmanuel¹, Eric P. Verrecchia⁸

¹: Sorbonne Université, CNRS-INSU, Institut des Sciences de la Terre Paris, IStEP, F-75005 Paris, France

²: CNRS, CReAAH, UMR 6566, Université de Rennes, F-35042 Rennes, France

³: Sorbonne Université, CNRS, EPHE, UMR 7619 METIS, F-75005 Paris, France

⁴: INRAP-Midi-Méditerranée, UMR 5068, TRACES, F-31000 Toulouse, France

⁵: University of Lausanne, Institut des Sciences de la Terre, CH-1015, Lausanne, Switzerland

⁶: Sorbonne Université, CNRS, Laboratoire d'Ecogéochimie des Environnements Benthiques, LECOB, F-66650, Banyuls, France

⁷: Géosciences Environnement Toulouse, CNRS, IRD, Université Paul Sabatier Toulouse 3, 14 Avenue Edouard Belin, F-31400 Toulouse, France

⁸: University of Lausanne, Institut des Dynamiques de la Surface Terrestre, CH-1015, Lausanne, Switzerland

*: Corresponding author: vmouchi@gmail.com; Current address: Sorbonne Université, CNRS, UMR 7144, Station Biologique de Roscoff, Place Georges Teissier, F-29680, Roscoff, France

ABSTRACT

Provenance determination of archaeological remains is a valuable tool for reconstruction of past exchange networks. Among these materials, oyster shells are ubiquitous in sites from all

24 prehistorical and historical periods. Thus, they seem to be as promising candidates for provenance
25 identification as they include chemical elements from the environment in their shells, which implies
26 that an elemental fingerprint of the region of origin can be recorded in the shell composition. In this
27 study, we present elemental measurements from 15 groups of modern and archaeological shells from
28 13 continental localities in mainland France and the island of Corsica (western Mediterranean Sea).
29 Two of these localities had two oyster species (*Crassostrea gigas* and *Ostrea edulis*). Results indicate
30 that (i) a species-specific elemental fingerprint exists and (ii) the Atlantic Ocean and Mediterranean
31 Sea provenances can be identified for *O. edulis* shells. Moreover, if the shell originated from a locality
32 only partially connected to the ocean (e.g. an estuary or lagoon), a fingerprint specific to the watershed
33 can also be observed, even between groups originating from the same bay. Using these measurements
34 as reference fingerprints, we characterize the Mediterranean origin of two groups of shells unearthed at
35 Lyons (central France, 200 km away from the nearest shoreline), dated from the 1st c. CE.

36

37 1. INTRODUCTION

38 Reconstruction of exchange networks in archaeology is paramount to study large-scale
39 medium- to long-term economics, as well as cultural and technological transfers, since routes were
40 vectors of ideas and cultural exchanges. Numerous studies have attempted to reconstruct the
41 provenance of marbles (Herz and Waelkens, 1988; Matthews, 1997; Mrozek-Wysocka, 2014),
42 obsidian (Robin et al., 2016; Kuzmin et al., 2018), variscite (Querré et al., 2015), ceramics (Michelaki
43 et al., 2013), and ore (Vogl et al., 2019). Yet, only a few studies have focused on shells and shell beads
44 from chemical analyses (Shackleton and Renfrew, 1970; Eerkens et al., 2005).

45 In Mesolithic and Neolithic sites from the European Atlantic seaboard, food wastes composed
46 of oyster shells are exclusively found on the coastline (Dupont, 2016) as the hunter-gatherer
47 populations consumed the soft body and discarded the shell on site. More recent sites from Antiquity
48 comprise oyster shells used for consumption in numerous localities, even distant from marine shores
49 (Bardot-Cambot, 2014). Indeed, during this period, oysters were consumed by the elite as delicacies

50 away from the sea (Bardot-Cambot, 2014). Most of the time, the provenance of these archaeological
51 shells remains unknown, unless these shells are associated with other taxa, (epi-)fauna, or substrate
52 that presents some endemic characteristics possibly identified by specialists (Schneider and Lepetz,
53 2007; Bardot-Cambot, 2013; Chaufourier et al., 2015; Somerville et al., 2017). However, these
54 identifications require substantial knowledge in cladistics as well as in the geological settings of the
55 shoreline at regional to country (even sometimes continental) scales, as it is known that high-level
56 dignitaries in Rome were used to import oysters from countries as far as England (Andrews, 1948;
57 André, 1981). In the more common case of non-endemic associated items, archaeologists rely on
58 morphometry to identify groups of shells of different origins (Gruet and Prigent, 1986a, 1986b;
59 Bardot-Cambot, 2014). Nonetheless, such characteristics are not specific to a locality but rather, to the
60 type of substrate (Gruet and Prigent, 1986a; Campbell, 2010; Somerville et al., 2017); therefore, they
61 are not relevant to the geographical identification of the specimen's origin beyond a single region.

62 Other techniques have been developed in order to identify the provenance of shell remains,
63 such as geochemical analyses, not only for archaeology (Eerkens et al., 2005, 2010; Mouchi et al.,
64 2020a), but also for quality control of modern cultured specimens prior to market distribution
65 (Bennion et al., 2019; Morrison et al., 2019). In addition, geochemistry has been used to study
66 connectivity of separated populations of mollusc species that colonize distant localities through larval
67 dispersion (Becker et al., 2005; Carson, 2010; Fodrie et al., 2011; Sorte et al., 2013).

68 Molluscs build their shells in calcium carbonate by sampling chemical elements from their
69 surrounding waters, and the shell's chemical composition reflects (at least partially) that of the
70 environment (Urey et al., 1951). Most studies have used oxygen and carbon stable isotope ratios ($\delta^{18}\text{O}$
71 and $\delta^{13}\text{C}$, respectively) from shells as a provenance proxy (Eerkens et al., 2005, 2010; Bajnóczi et al.,
72 2013; Milano et al., 2019; Apolinarska and Kurzawska, 2020), but the use of this approach appears to
73 be restricted to differentiate between marine and brackish/estuarine environments. Indeed, $\delta^{18}\text{O}$ and
74 $\delta^{13}\text{C}$ are mainly representative of local biogeochemical conditions rather than the geographical
75 location (temperature and salinity for $\delta^{18}\text{O}$ and food source for $\delta^{13}\text{C}$; Craig, 1965; Sharp, 2007;
76 Lartaud et al., 2010a). Temporal homogeneity for the regional fingerprint cannot be insured as

77 seasonal temperatures have an impact on $\delta^{18}\text{O}$, leading to the overlap of amplitude values with remote
78 areas exhibiting similar seasonal temperature contrasts (Mouchi et al., 2020b). Additionally, it was
79 recently demonstrated that oysters do not mineralize their shell in equilibrium with seawater during
80 their first year of growth, making unlikely the use of $\delta^{18}\text{O}$ as a proxy for local physicochemical
81 conditions during this life stage (Huyghe et al., 2020). Overall, elemental analyses tend to provide
82 better results in provenance determination than carbon and oxygen isotopic compositions (Zhao and
83 Zhang, 2016; Ricardo et al., 2017; Bennion et al., 2019; Morrison et al., 2019). Nevertheless, such
84 studies have identified issues related to ‘vital effects’: the metabolism acts as a filter between the
85 living environment and the shell, thus modifying the shell’s final composition. It has indeed been
86 shown (Mouchi et al., 2020a) that concentrations in rare earth elements (REE) can be used to identify
87 the region of provenance for the cupped oyster *Crassostrea gigas*. Still, these elements are not
88 discriminant for the flat oyster, *Ostrea edulis*, which is the only oyster species found in European
89 archaeological sites, as the cupped oyster *Crassostrea angulata* was imported to Portugal from Asia
90 during the 17th century. Consequently, other chemical elements need to be investigated as provenance
91 proxies for *O. edulis*.

92 In the present study, we use a new multi-elemental approach based on laser-ablation
93 inductively-coupled plasma mass spectrometry (LA-ICP-MS) performed on 68 modern and
94 archaeological oyster specimens (*C. gigas* and *O. edulis*) from 15 groups of different localities and
95 ages. We aim at using this approach to identify potential discriminant elements for provenance studies
96 applied to both oyster species found in Europe. This technique was selected as it is fast and commonly
97 used in carbonate geochemistry studies (Durham et al., 2017).

98

99 2. MATERIALS AND METHODS

100 **2.1. Collection sites and specimens**

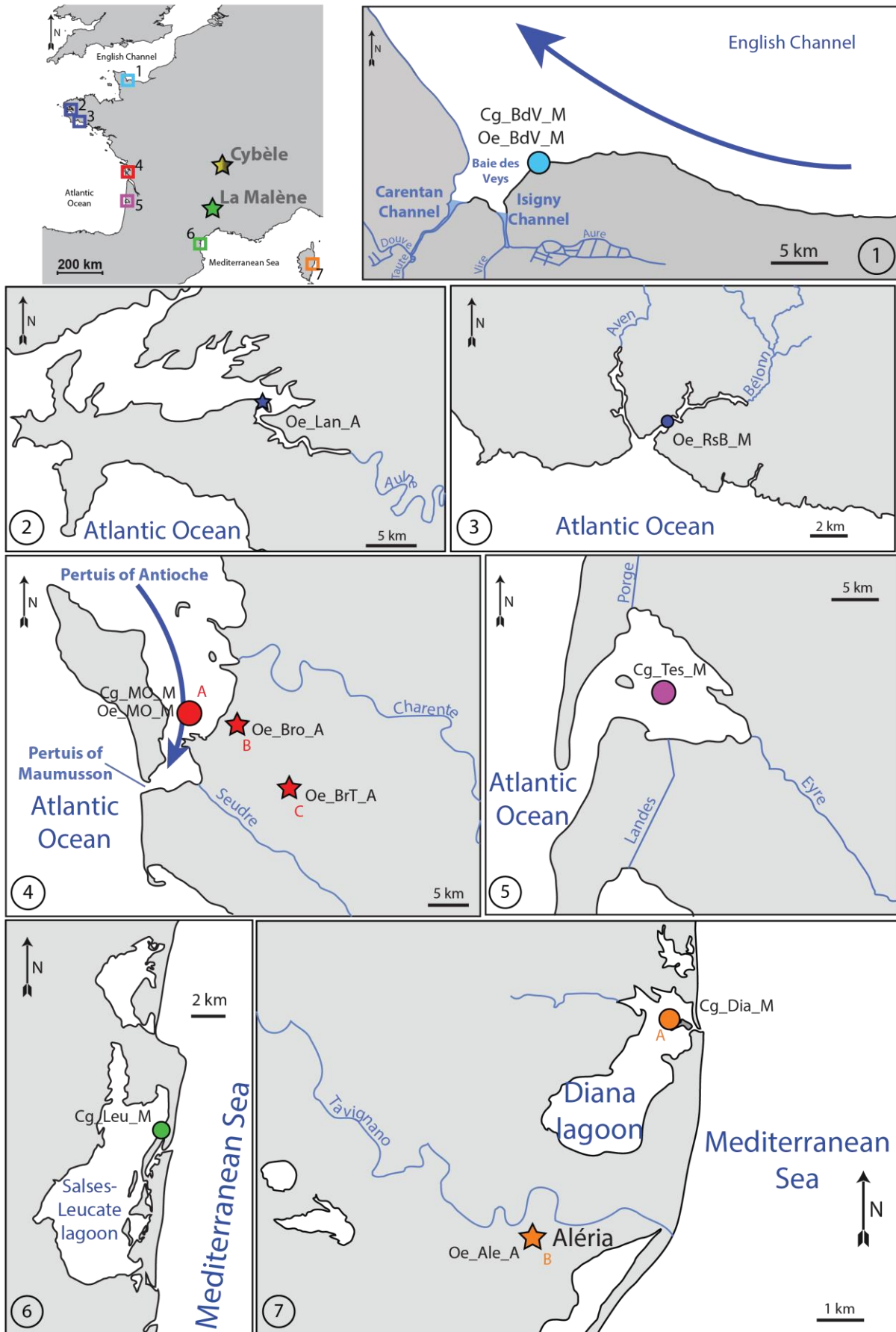
101 Samples were collected from multiple modern localities and archaeological sites in continental
102 France and the island of Corsica (**Figure 1; Table 1**). As elemental composition of the rivers

103 (suggested to influence the composition of seawater and shells at the output) reflects the composition
 104 of substrate weathered on land, a brief description of the geological formations of watersheds are
 105 indicated with site descriptions in **Supplementary Information 1**. Specimens are divided into groups
 106 of origin, according to their species ('Cg' and 'Oe' for *C. gigas* and *O. edulis*, respectively), their
 107 locality (see **Table 1**), and their age ('M' for modern and 'A' for ancient specimens). Although the
 108 species *Crassostrea gigas* has been recently renamed *Magallana gigas* (Salvi and Mariottini, 2016),
 109 this genus change is debated by numerous experts (Bayne et al., 2017), so we will continue to use the
 110 name *Crassostrea gigas* throughout the paper.

111 **Table 1:** Number of specimens and measurements per group of shells.

Group	Location	Coordinates	ID on Figure 1	Age	Number of specimens	Number of measurements
Cg_BdV_M	Baie des Veys (Normandy)	49°23.11 N, 01°06.05 W	1	Modern	5	38
Oe_BdV_M	Baie des Veys (Normandy)	49°23.11 N, 01°06.05 W	1	Modern	5	38
Oe_Lan_A	Landévennec (Brittany)	48°17.42 N, 04°16.00 W	2	8 th – 15 th c. CE	2	16
Oe_RsB_M	Riec-sur-Bélon (Brittany)	47°48.55 N, 03°43.08 W	3	Modern	3	20
Cg_MO_M	Marennes-Oléron (Charente-Maritime)	45°52.23 N, 01°10.60 W	4A	Modern	3	23
Oe_MO_M	Marennes-Oléron (Charente-Maritime)	45°52.23 N, 01°10.60 W	4A	Modern	3	16
Oe_Bro_A	Brouage (Charente-Maritime)	55°85.05 N, 01°07.44 W	4B	16 th c. CE	4	24
Oe_BrT_A	Broue tower (Charente-Maritime)	45°47.67 N, 00°58.57 W	4C	11 th – 14 th c. CE	6	40
Cg_Tes_M	Tès (Arcachon Basin)	44°40.01 N, 01°08.18 W	5	Modern	8	70
Cg_Leu_M	Leucate (Aude)	42°52.48 N, 03°01.50 E	6	Modern	5	35
Cg_Dia_M	Diana lagoon (Corsica Island)	42°08.00 N, 09°32.17 E	7A	Modern	2	13
Oe_Ale_A	Aléria (Corsica Island)	42°06.50 N, 09°30.72 E	7B	Antiquity	2	14
Oe_X1_A	Unknown	Unknown	-	1 st c. CE	6	45
Oe_X2_A	Unknown	Unknown	-	1 st c. CE	8	41
Oe_Mal_A	Undefined (Mediterranean Sea)	Unknown	-	6 th c. CE	6	39

112



114 **Figure 1:** Sample collection sites. Modern specimen groups are indicated by circles while archaeological specimen groups
115 are presented as stars. Colour coding corresponds to that used in the t-SNE analysis on the following figures. 1: Baie des
116 Veys modern site. Arrow: direction of the English Channel current near the shore (Lazure and Desmare, 2012). 2:
117 Landévennec Medieval site. 3: Riec-sur-Bélon modern site. 4: Charente-Maritime, comprising the modern site of Marennes-
118 Oléron (A), the Renaissance site of Brouage (B), and the Medieval site of Broue tower (C). Arrow: direction of the current in
119 the bay (Dechambenoy et al., 1977). 5: Tès modern site. 6: Leucate modern site. 7: Corsica island sites, comprising the
120 modern site of Diana lagoon (A) and the Antiquity site of Aléria (B). Additional archaeological groups are the Medieval
121 shells found at La Malène of confirmed Mediterranean origin and two groups unearthed at Cybèle (Lyons) of unknown
122 origin.

123

124 **2.2. Sample selection and preparation**

125 The preparation protocol is given in Mouchi et al. (2020a). Multiple specimens were selected
126 from each group based on the apparent preservation of the umbo region of the shell. Epibionts, when
127 present, were mechanically removed. The umbo of the left valve was embedded in Huntsman Araldite
128 2020 epoxy resin, cut through using a Buehler low-speed saw to expose the preserved internal
129 structures along the growth axis, and made into polished 750 µm-thick sections. As the umbo records
130 the entire growth of the shell in a condensed area, geochemical analyses on such sections have the
131 benefit of being deprived of surface contaminations of chemical or organic origin (Richardson et al.,
132 1993; Kirby et al., 1998). Indeed, the umbo is a dense area, protected from the exterior environment
133 within the bivalve, which generally presents a much better preservation compared to the rest of the
134 shell. In addition, oyster shells are made of lamellae that can be intertwined with empty spaces that can
135 be filled with organic and sedimentary contaminants, which could strongly interfere with the quality of
136 the measurements.

137 Each section was observed under cathodoluminescence to ensure the pristine state of the
138 surface and to outline the seasonal calibration of the shell based on the intensity of luminescence
139 (Lartaud et al., 2010b; Mouchi et al., 2018; Huygue et al., 2019). Following the growth direction, areas
140 of strong luminescence correspond to parts of the shell built in summer periods, while areas in dull
141 luminescence have grown during winter periods. Observations were completed using a Cathodyne-

142 OPEA cold cathode at ISTE_P, Sorbonne Université (Paris, France) with 15-20 kV, 200-400 $\mu\text{A}\cdot\text{mm}^{-2}$
143 and a pressure of 0.05 Torr. Shells from Leucate (Cg_Leu_M) were the only specimens that did not
144 exhibit cathodoluminescence, which made the seasonal calibration impossible. The seasonal
145 calibration from morphology proposed by Kirby et al. (1998) was also unsuccessful due to the absence
146 of the necessary curved surface of the umbo. All specimens from the other groups were seasonally
147 calibrated.

148 **2.3. Geochemical analyses by LA-ICP-MS**

149 Measurements were performed using an Element XR (ThermoScientific) ICP-MS coupled
150 with a RESOLUTION 193 nm ArF excimer ablation system equipped with an S155 two-volume ablation
151 cell (Australian Scientific Instruments) at ISTE (University of Lausanne, Switzerland). The analyses
152 were carried out with a pulse repetition rate of 20 Hz and an on-sample energy density of 4 $\text{J}\cdot\text{cm}^{-2}$.
153 Sample areas were cleaned from potential surface contamination (during polishing) by conducting pre-
154 ablation. Spot size was 200 μm . Measurements were conducted on both summer and winter zones,
155 based on the seasonal calibration. Measurements on Leucate specimens (Cg_Leu_M) were positioned
156 randomly instead. Each specimen (shell) was measured several times in order to avoid bias due to
157 internal variability. We carefully avoided performing measurements in suspicious areas regarding
158 preservation, based on cathodoluminescence observation. We performed at least two adjacent
159 measurements for each selected season area, with generally six to eight measurements per shell
160 (sometimes less, *e.g.* four measurements for some Oe_MO_M specimens, due to lower growth rates
161 restricting the surface available for measurements). For most specimens, three to four successive
162 season areas were sampled. Prior and following each 15-sample series, NIST SRM 612 was measured
163 for external calibration. Accuracy of the analyses was checked against measurements of the BCR-2
164 basalt reference material from USGS according to the GeoReM preferred values (Jochum et al., 2005).
165 Relative standard deviation for all measured elements range from 1.2 % to 5.8 % (**Supplementary**
166 **Information 2**). Measured elements were La, Ce, Pr, Nd, Sm, Ti, Cr, Cu, Zn, Sr, Ba, Pb, U, Y, and Ca
167 as the internal standard. Data reduction was performed using the LAMTRACE software (Jackson,
168 2008). A total of 472 measurements were acquired.

169 2.4. **Data processing**

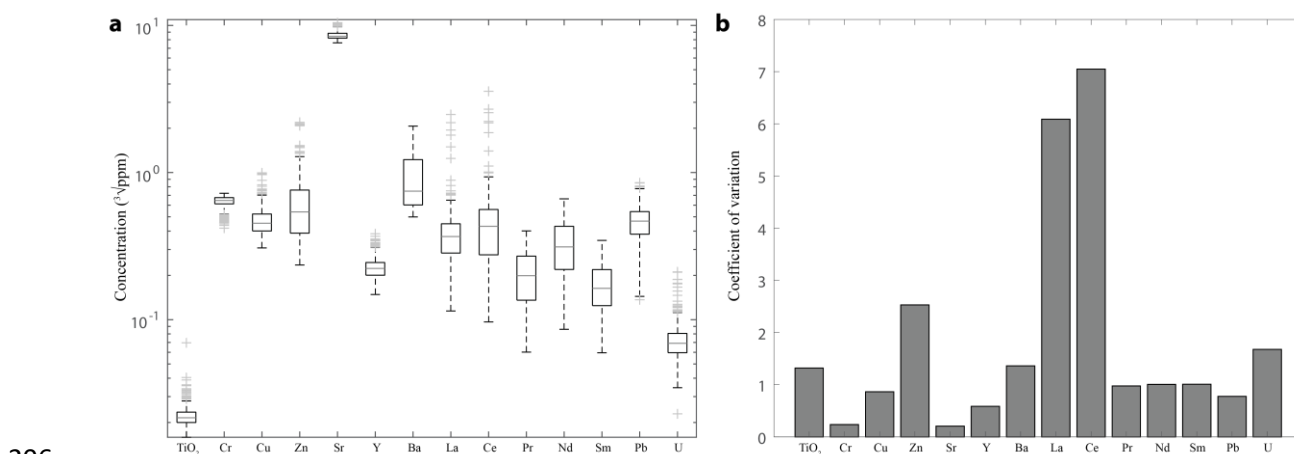
170 All data processing was conducted using the Matlab software (MathWorks,
171 www.mathworks.com, v. R2017a). As none of the 14 measured elements presented a normal
172 distribution (Kolmogorov-Smirnov test) due to a right-skewed distribution (towards larger element
173 abundances), it was necessary to transform the data to normality for statistical processing, which was
174 performed by using the cubic root transform (Chen and Deo, 2004). Hierarchical cluster analyses were
175 used to estimate seasonal differences (using the seasonal age models based on the
176 cathodoluminescence signal) at Baie des Veys on 38 measurements from *C. gigas* specimens
177 (Cg_BdV_M; n=5) and 38 measurements from *O. edulis* specimens (Oe_BdV_M; n=5), and at
178 Marennes-Oléron on 23 measurements from *C. gigas* specimens (Cg_MO_M; n=3) and 16
179 measurements from *O. edulis* specimens (Oe_MO_M; n=3). Two methods were tested: unweighted
180 average distance and “Ward” inner squared distance. The cophenetic correlation coefficient between
181 the distances obtained from the cluster tree and the original distances (in the multivariate space) is an
182 indicator of the quality of the estimation (of the hierarchical cluster analysis) to faithfully represent
183 dissimilarities between observations being compared. Comparison and classification between all
184 groups were performed using t-SNE (t-distributed Stochastic Neighbour Embedding; van der Maaten
185 and Hinton, 2008) with the exact Euclidean method. This method allows high-dimensional data points
186 to be imbedded in low dimensions (typically two dimensions) in a way that respects similarities
187 between points: distant points in a high-dimensional space correspond to distant embedded low-
188 dimensional points, and nearby data points in the high-dimensional space correspond to nearby
189 embedded low-dimensional points (MathWorks, www.mathworks.com, v. R2017a). In other words,
190 each point represented by t-SNE corresponds to the overall composition of one measurement of all 14
191 elements, two close points having a similar composition while two distant points reflect different
192 compositions. To prevent the undesirable over-influence of some elements showing wide variance, we
193 performed t-SNE on normalized data. The Matlab script for t-SNE processing is available as
194 **Supplementary Information 3**. As we focus on comparing the concentrations between individual
195 shells from multiple localities using the same (LA-ICP-MS) analytical method, the host phase (organic

196 or mineral) of specific elements and their resulting co-variations within a measurement are not
197 discussed here.

198

199 3. RESULTS

200 All measurement results are presented in **Figure 2a**. The three elements with the largest
201 coefficients of variation are Ce, La and Zn, followed by U, Ba, and Ti (**Fig. 2b**). All other elements
202 appear to have a low variance in the dataset. Except for Sr, Ba, Zn, La, and Ce, all measured elements
203 have concentrations below 1 ppm. Boxplots by element for all the shell groups are provided as
204 **Supplementary Information 4**. None of the elements can be used to differentiate between the origins
205 of the various groups on its own.

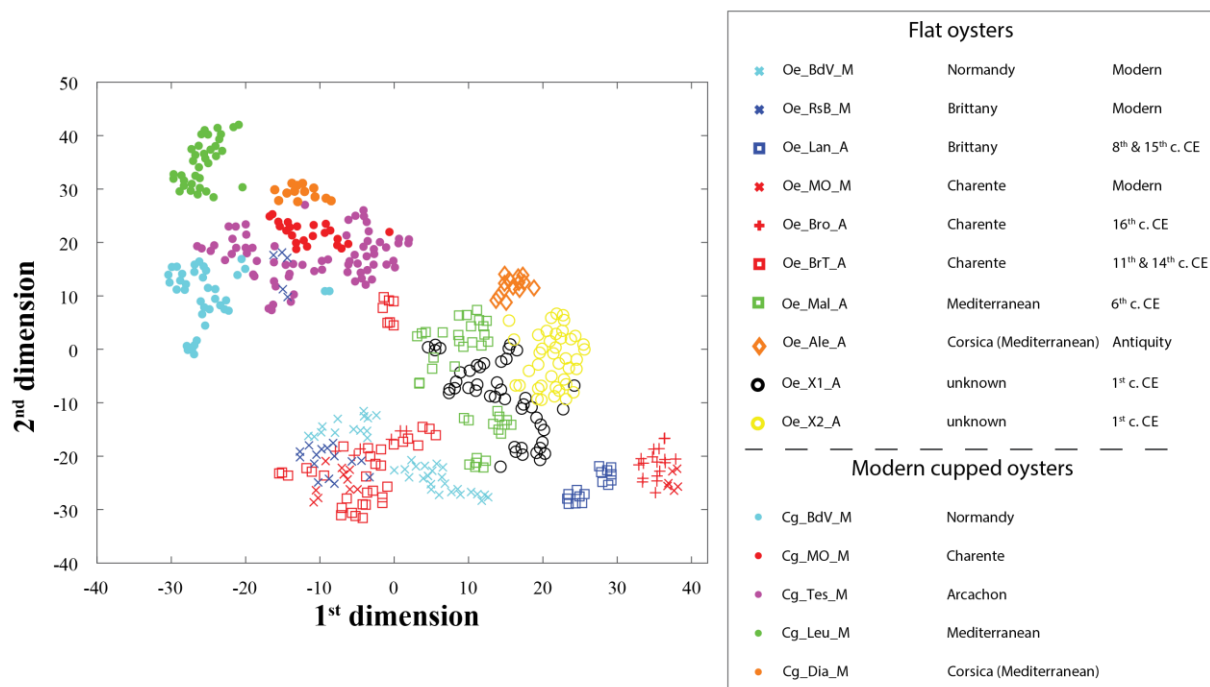


207 **Figure 2:** Distribution of the 472 measurements for each analyte. **a:** Boxplot with values indicated in cubic root for best
208 approaching the normality in the distribution and for clarity. Note that the ordinate axis is in logscale. **b:** Coefficient of
209 variation for each analyte.

210

211 Similarities and differences between the 15 shell groups based on geochemical data are plotted
212 in **Figure 3** using t-SNE. First, the five groups of *C. gigas* shells are positioned at the upper left side of
213 the figure, while *O. edulis* samples are spread out in a much wider area. Moreover, the measurements
214 performed on both species from the same site (*i.e.*, Cg_BdV_M and Oe_BdV_M for Baie des Veys,
215 and Cg_MO_M and Oe_MO_M for Marennes-Oléron) do not overlap, indicating that the

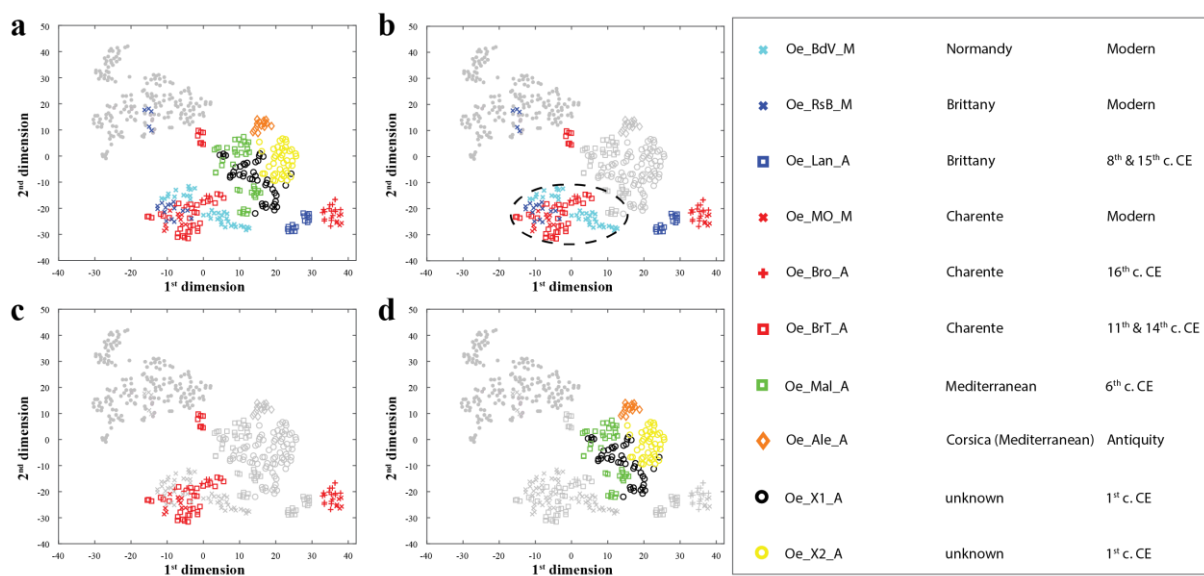
216 compositions of the shells are not identical for both species from the same locality. Furthermore, the
 217 five groups of *C. gigas* shells are relatively well identified, particularly those of Leucate (Cg_Leu_M),
 218 Diana lagoon (Cg_Dia_M) and Baie des Veys (Cg_BdV_M). The Marennes-Oléron (Cg_MO_M) and
 219 Tès (Cg_Tes_M) groups partially overlap.



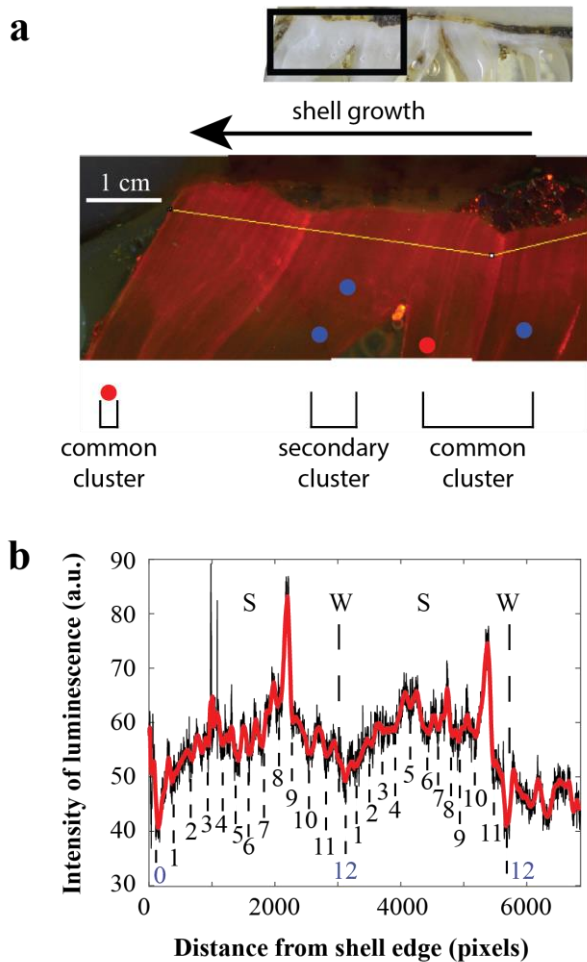
220
 221 **Figure 3:** Visualization of shell groups' partitioning using t-SNE (exact method using Euclidean distance) based on 472
 222 measurements. *Crassostrea gigas* shell measurements are indicated with dots. Light blue symbols represent measurements
 223 from shells originating from Normandy, dark blue symbols represent Brittany, red symbols represent Charente, purple
 224 symbols represent Arcachon Basin, and green and orange symbols represent the Mediterranean Sea, including Corsica. Two
 225 groups of Antiquity shells of unknown origin are indicated by yellow and black circles.

226
 227 Although some *O. edulis* groups are well defined without any measurement overlap from other
 228 groups (*i.e.*, Oe_Ale_A and Oe_Lan_A), some groups of this species are more difficult to discriminate
 229 geochemically (**Figure 4a**). Indeed, when only considering groups originating from localities on the
 230 English Channel and the Atlantic Ocean coastlines (*i.e.*, open seas with strong tidal influence),
 231 numerous measurements cluster without discrimination between the locality of origin (dashed ellipse
 232 in **Figure 4b**). Only the Landévennec (Oe_Lan_A) group is absent from this common cluster.
 233 Inversely, the Oe_BdV_M group measurements are found solely in this common cluster. For the

234 Oe_RsB_M, Oe_MO_M, Oe_Bro_A and Oe_BrT_A groups, other measurements are found in
 235 ‘secondary’ clusters in addition to their presence in the common cluster, which are specific to the
 236 group. Some specimens from these groups have a unique fingerprint corresponding to one or the other
 237 cluster (common or secondary), while other specimens have fingerprints corresponding to both
 238 clusters along successive measurements, following shell growth (**Figure 5**). Amongst them,
 239 Oe_MO_M and Oe_Bro_A (both from Charente-Maritime) share this ‘secondary cluster’, while Broue
 240 tower (Oe_BrT_A; from the Charente-Maritime region as well) has a ‘secondary cluster’ isolated from
 241 the others (**Figure 4c**). It is also worth noting that specimens from the Oe_BrT_A group, which have
 242 been collected from two distinct temporal units in the site (see **Supplementary Information 1**),
 243 present measurements in the common cluster as well as in the secondary cluster for specimens from
 244 both stratigraphic units (sometimes along the same specimen), confirming that the local elemental
 245 fingerprint is identical over centuries. However, the two specimens from Landévennec (Oe_Lan_A),
 246 belonging to two different temporal periods, are discriminated from one another by t-SNE (**Figure 3**)
 247 in the form of two groups of measurements in the Landévennec cluster.



248
 249 **Figure 4:** Visualization of *O. edulis* shell groups’ partitioning using t-SNE showing specific groups. **a:** t-SNE from Figure 3
 250 with measurements from *C. gigas* shells shaded. **b:** Same as **a** showing only groups of confirmed English Channel or Atlantic
 251 Ocean coastlines. The dashed ellipse indicates a cluster common to measurements from several groups. **c:** Same as **a** showing
 252 only the three Charente groups. **d:** Same as **a** showing only the groups from the Mediterranean coastline and the two groups
 253 of unknown origin.



254

255 **Figure 5:** Successive measurements along shell growth indicating different fingerprints on specimen 1297-2 from Broue
 256 tower (Oe_BrT_A), namely “common cluster” and “secondary cluster” on Fig. 4b. **a:** Cathodoluminescence view of the last
 257 two years of growth (corresponding to the area analysed by LA-ICP-MS) on the umbo region and positions of the
 258 measurements. Red and blue dots correspond to summer and winter measurements, respectively. Note that the first
 259 measurement on the left is out of the picture frame. **b:** Intensity of luminescence (in arbitrary units) along the umbo following
 260 the line indicated on **a**, showing the areas of light (corresponding to summers; “S”) and dull (corresponding to winters; “W”)
 261 luminescence. Smoothing of this signal is shown overlapping in red, and highlights the presence of a monthly tidal cycle
 262 (numbers).

263 When considering the two remaining groups of confirmed origin, both from the Mediterranean
 264 Sea (an enclosed basin with a narrow opening to the Atlantic Ocean through the Strait of Gibraltar),
 265 each group is defined by a single cluster without any overlap (in green and orange in **Figure 4d**). The
 266 measurements from the groups of unknown origin overlap at least partially with the Oe_Mal_A group.

267 Data collected from specimens bred at Baie des Veys and Marennes-Oléron were used to
268 study the differences between seasons for both species based on dendrograms (**Supplementary**
269 **Information 5**). Seasons cannot be reliably discriminated, as indicated by the cluster analyses that
270 show both seasonal measurements mixed together. For Cg_BdV_M, the cophenetic correlation
271 coefficients are 0.80 and 0.52 for average and Ward methods, respectively. In the same site, for
272 Oe_BdV_M, coefficients are 0.89 and 0.77 for average and Ward methods, respectively. Similar
273 cophenetic correlation coefficients are found for Cg_MO_M with 0.70 and 0.62 for average and Ward
274 methods, respectively, and for Oe_MO_M with 0.89 and 0.77 for average and Ward methods,
275 respectively. The identification of seasons for all the measurements (except Leucate specimens; see
276 section 2.2) in the t-SNE distribution is also reported in **Supplementary Information 5**.

277

278 4. DISCUSSION

279 **4.1. Large-scale provenance discrimination**

280 It was previously reported that REE and Y cannot be used for *O. edulis* as a provenance proxy
281 due to vital effects, unlike *C. gigas* (Mouchi et al., 2020a). Consequently, other elements were
282 investigated in this study in order to provide a potential regional fingerprint for this species and to find
283 a way to efficiently compare measurements from *O. edulis* and *C. gigas* in terms of sourcing. The
284 results show that REE are not the only elements whose incorporation differ between these two species.
285 Indeed, the Cg_BdV_M and Oe_BdV_M groups, which originate from the same modern locality (and
286 reared simultaneously on the same culture table in Baie des Veys, Normandy), exhibit obvious
287 different compositions (**Figure 3**). Observations are similar for Cg_MO_M and Oe_MO_M from
288 Marennes-Oléron, Charente-Maritime. However, it seems possible, when considering only one of the
289 two species, to discriminate the composition depending on their region of origin, if not the locality.

290 For *C. gigas* specimens, the shells from the Mediterranean Sea (Cg_Leu_M and Cg_Dia_M),
291 seem to be separated by t-SNE from the Atlantic Ocean/English Channel groups along the second
292 dimension (approximately around unit 25 in **Figure 3**). This separation appears to be controlled by a

293 lower abundance in light REE in the Mediterranean groups compared to the Atlantic groups
294 (**Supplementary Information 4**). This low abundance in light REE can either be specific to the
295 Mediterranean shells or to the relatively small watersheds from these two localities (the smallest of the
296 entire dataset). Although most of the Baie des Veys measurements are discriminated by t-SNE from
297 other groups, some measurements share their composition with a part of the Tès group (Cg_Tes_M),
298 which itself is partially connected to the Marennes-Oléron group (Cg_MO_M). This observation tends
299 to indicate that specimens from the English Channel (Baie des Veys) and the Atlantic Ocean
300 (Marennes-Oléron and Tès) exhibit some similarities in their geochemical composition.

301 For *O. edulis*, the common cluster (dashed ellipse in **Figure 4b**) gathers measurements from
302 specimens from the Atlantic Ocean and English Channel coastlines, covering roughly 700 km of
303 coastline (**Figure 1**) from Charente-Maritime in the south (Oe_MO_M, Oe_Bro_A, Oe_BrT_A) to
304 Normandy in the north (Oe_BdV_M). As the English Channel and the Atlantic Ocean are connected
305 across a wide area, the overall composition of seawater should share some similarities. On the
306 contrary, the Mediterranean Sea is a semi-enclosed basin and is recharged by the Atlantic Ocean
307 through the narrow Strait of Gibraltar. A difference in composition is expected in shells from
308 Mediterranean localities. In addition, the near absence of tidal range in this region compared to the
309 Atlantic Ocean can cause differences in fluid mixing and elemental incorporation in the shells.
310 Therefore, it appears possible to discriminate, at a large scale, between specimens from the Atlantic
311 Ocean/English Channel and the Mediterranean Sea.

312 **4.2. Fine-scale provenance discrimination**

313 The common cluster composed of samples from Oe_BdV_M, Oe_RsB_M, Oe_MO_M,
314 Oe_Bro_A, and Oe_BrT_A shells (Baie des Veys: Normandy; Riec-sur-Belon: Brittany; Marennes-
315 Oléron, Brouage and Broue tower: Charente) represents a homogenous fingerprint. These groups are
316 from watersheds with quite distinct geological formations (limestones, basalts, etc...) but share a large
317 seawater body (*i.e.*, the Atlantic Ocean). However, we observe that each group in this cluster has also
318 a secondary cluster outside the common one, which seems group-specific, except for the Baie des
319 Veys (Oe_BdV_M; **Figure 4b**). Within these groups, some specimens have all their measurements

320 within a single cluster (either the common cluster or the secondary cluster of the corresponding
321 group), while other specimens have some measurements in both clusters (**Figure 5**). As these
322 specimens have not been transferred from one location to another during growth, it appears that these
323 changes in elemental incorporation occurred over the growth of the organism in the same site. As
324 these changes occur multiple times over the growth period (**Figure 5**), it cannot be caused by
325 ontogeny. This cyclical pattern is not linked to seasonality (this was checked by the seasonal
326 calibration using cathodoluminescence; see t-SNE figure in **Supplementary Information 5**).
327 Consequently, a different factor is at play. Temporal resolution of the LA-ICP-MS measurements is
328 approximately one month, based on a tidal cathodoluminescence signal (Mouchi et al., 2013; see
329 monthly cycles on **Figure 5b**) and *in vivo* labelling (Lartaud et al., 2010b; **Supplementary**
330 **Information 6**). Growth rates can however be different according to the specimen and the period
331 considered, and some measurements may represent a slightly shorter or longer period (Huyghe et al.,
332 2019). Since all the corresponding groups originate from the English Channel and the Atlantic Ocean
333 shorelines, tidal influence can be a pertinent factor. Indeed, all the groups from the Mediterranean Sea
334 (Oe_Mal_A, Oe_Ale_A), which exhibits a very weak tidal range (only a few centimetres), are
335 excluded from the common cluster (**Figure 4d**). In localities with a broad tidal range, the influence of
336 the chemistry of nearby rivers could fluctuate widely, increasing during low tide and, on the contrary,
337 being diluted with seawater at high tide. If this were the case, the secondary clusters would represent
338 the correct local fingerprint, while the common cluster would correspond to the fingerprint of Atlantic
339 seawater. Manganese is known to fluctuate in oyster shells from ebb to flood currents (Huyghe et al.,
340 2019). Other chemical elements (*e.g.* those measured here) could present similar fluctuations.
341 Switching between these two compositions, which are responsible for the presence of two distinct
342 fingerprints, could be caused by the relative proportion (by volume in the analysed shell) of carbonate
343 formed during ebb and flow currents. The proportion may vary, depending on growth rates. The case
344 of the Baie des Veys shells (Oe_BdV_M group) is singular as it has no secondary cluster (**Figure 4b**).
345 Interestingly, this site is also the locality with the most open marine settings from all modern groups.
346 Although some shells of other groups did not have measurements corresponding to secondary clusters,
347 the fact that no measurements from the 38 performed on five specimens are outside this common

348 cluster would tend to imply that there is only one fingerprint in this site. This observation is supported
349 by the marine water mass current of the Baie des Veys, which flows towards the direction of the
350 rivers' outputs from the locality where the oysters were collected (**Figure 1**; Lazure and Desmare,
351 2012), hence limiting the influence of the composition of the freshwater coming from the land. Becker
352 et al. (2005) measured the elemental fingerprint of young mussel shells in several localities in San
353 Diego County to study the larval dispersal along the coastline. They were able to observe distinct
354 fingerprints for specimens from estuarine locations, but could not clearly discriminate open marine
355 locations. We suspect this is what is observed here, with a 'marine' fingerprint common to several
356 groups (being identical to that of an open marine locality, *i.e.* Baie des Veys), and a secondary
357 fingerprint, specific to the locality, in environments where continental inputs are sufficiently strong.
358 This assumption is supported by a higher and more stable salinity in Baie des Veys (approximately 33
359 all year) than in Marennes-Oléron (27 to 34; Lartaud et al., 2010c).

360 Temporal changes in the local elemental fingerprint have already been reported in mollusc
361 shells, such as *Cerastoderma edule* and *Mytilus edulis* from Ireland (Ricardo et al., 2017; Bennion et
362 al., 2019). These differences occur within months and observations in this study confirm that it is also
363 the case for *O. edulis*, although the same is not true for *C. gigas*. These differences appear to switch
364 back and forth between two fingerprints (**Figure 5**), one being common to multiple groups of shells of
365 various origins in the French Atlantic Ocean and English Channel coastlines.

366 The case of the Charente-Maritime groups (Marennes-Oléron: Oe_MO_M; Brouage:
367 Oe_Bro_A; and Broue tower: Oe_BrT_A) is interesting, as two distinct secondary clusters are visible
368 in the t-SNE plot (**Figure 4c**). One of these groups of shells has been collected in the present day
369 (Marennes-Oléron) with the exact location known, while the two other groups (Brouage and Broue
370 tower) have been found in archaeological sites on land, with evidence that these locations were on the
371 shoreline at the corresponding ages of the specimens. The fingerprint of the modern group is shared by
372 the Brouage group dated from the 16th century CE (Oe_Bro_A). On the contrary, the Broue tower
373 shells from the 11th and the 14th centuries CE (Oe_BrT_A) present a distinct fingerprint. It may be
374 possible that the oysters from this group were living in a locality in the region under the influence of

375 another freshwater flow with a different water composition. Indeed, the Marennes-Oléron bay has two
376 major tributary rivers, which cross different geological formations, although the main rock type is
377 limestone (Bourgueil et al., 1968, 1972; Platel et al., 1977, 1978; Bambier et al., 1982; Hanztpergue et
378 al., 1984; Mourier et al., 1989). The site of Brouage, from which were unearthed the shells of the
379 Oe_Bro_A group, is located at the same level in the bay as the modern Marennes-Oléron group
380 (Oe_MO_M; Champagne et al. 2012; **Figure 1**), with which it shares its secondary cluster. The site of
381 the Broue tower, where the shells from the Oe_BrT_A group were discovered, is located further south,
382 near the current output of the Seudre river (**Figure 1**; Normand et al., 2019). As seawater currents
383 cross the bay from north to south, the oysters from the Oe_MO_M and Oe_Bro_A groups must have
384 been under the influence of the Charente River (north side of the bay), but not the Seudre River. On
385 the contrary, specimens from the Oe_BrT_A group must have been mainly under the influence of the
386 Seudre River. The measurements show that, in such contexts, the identification of the region can be
387 narrowed down to the watershed level. In addition to this, although temporal differences in local
388 elemental fingerprints have been reported in other regions (Ricardo et al., 2017; Bennion et al., 2019),
389 the fact that both modern (Oe_MO_M) and ancient (Renaissance, Oe_Bro_A) shells share a common
390 cluster and a local cluster over the course of several centuries indicate that multiple measurements
391 over the growth direction of shells can allow the local elemental fingerprint to be recognized, whatever
392 the period of collection. This interpretation is also supported by the Oe_BrT_A specimens, which
393 present fingerprints corresponding to both the common cluster and the same (locality-specific)
394 secondary cluster, whether specimens are from the 11th or the 14th c. CE.

395 The only group of shells from the English Channel/Atlantic Ocean coastline that have no
396 measurements corresponding to the common cluster is Oe_Lan_A. The Medieval site at Landévennec,
397 from which these shells were unearthed, is located in the direct proximity of the Aulne River (**Figure**
398 **1**). Although the salinity is close to marine (generally around 32 except during flooding events where
399 salinity drops to 15; Monbet and Bassoulet, 1989), the river rate of flow (annual mean of 24 m³.s⁻¹;
400 Auffret, 1981) is probably high enough to induce a strong influence in terms of chemical composition
401 of the local seawater. That way, even at high tide, the composition of shells, derived from the local

402 seawater, would still be substantially influenced from the Aulne River. The two sub-groups from this
403 cluster, with each corresponding to one specimen of different age (8th and 15th centuries CE), are
404 probably due to a different degree of the influence of freshwater input. As several centuries separate
405 these specimens, it is probable that the local geomorphology and water level changed, causing
406 relocation of the supply of oysters from the inhabitants. Nevertheless, the close similar fingerprint of
407 these specimens implies that they originate from nearby locations.

408 For *C. gigas* groups, all measurements from the Cg_Leu_M group of shells are clustered away
409 from the other groups in **Figure 3**, with highly negative values on the 1st dimension axis and highly
410 positive values on the 2nd dimension axis. This observation indicates that the elemental compositions
411 of these shells are substantially different than the shells from the other regions. The fingerprint from
412 the Diana lagoon (Cg_Dia_M) is also easily discriminated from the others. Compared to the other
413 regions, these localities are characterized by small watersheds, uniquely consisting in limestone. As
414 one can expect a smaller surface exposed to weathering than those of the other studied localities, the
415 abundance of some elements in the shell should be lower at Leucate and Diana lagoon. Indeed, both
416 groups are characterized by low abundances of light REE compared to the other groups, but the other
417 analysed elements do not present such a systematic lower content (**Supplementary Information 4**). It
418 is also possible that, as both these localities are in restricted lagoons, salinity can be at play. Indeed,
419 Diana Lagoon (Mediterranean Sea) is known to have a high salinity (37.3 annual mean; Orsini et al.,
420 2001) and Leucate lagoon has a seasonally dominated salinity (26 in winter and 42 in summer due to
421 evaporation; Andrisoa et al., 2019), whereas Baie des Veys and Marennes-Oléron (Atlantic coastline)
422 have lower salinities (33.4 and 32.4 annual mean, respectively; Lartaud et al., 2010c).

423 For “Atlantic Ocean” *C. gigas* specimens, the Baie des Veys group (Cg_BdV_M; although
424 situated in the English Channel, with a wide access to the Ocean) appears to be the most distinct by t-
425 SNE between these groups, with only some measurements overlapping with the Tès group. This is
426 interesting, as *O. edulis* shells from the same locality (Oe_BdV_M) had the peculiar characteristic of
427 representing the composition of a cluster common to other Atlantic groups. The Tès (Cg_Tes_M) and
428 Marennes-Oléron (Cg_MO_M) groups share their distribution in the t-SNE graph, with the Marennes-

429 Oléron distribution entirely comprised into a restricted portion of the Tès distribution. The large
430 distribution by t-SNE of Tès measurements compared to Marennes-Oléron can be explained by the
431 annual range of salinity (approx. 15 and 5, respectively for Tès and Marennes-Oléron; Lartaud et al.,
432 2010c). These two localities (Arcachon Basin and Charente-Maritime) have their watersheds crossing
433 different geological formations with mainly Cenozoic river deposits for Tès (Dubreuilh et al., 1992)
434 and mainly Mesozoic limestone for Marennes-Oléron (Bourgueil and Moreau, 1967, 1970; Bourgueil
435 et al., 1968; Platel et al., 1977; 1978). Still, the deposit cover of the respective watersheds does not
436 appear to be sufficient to entirely discriminate these groups.

437 **4.3. Attempting to identify the provenance of the Lyons/Cybèle shells**

438 The Oe_Mal_A group from La Malène belongs to a specific locality, which is unknown, but at
439 least confirmed from the Mediterranean coastline, probably from Languedoc coastline due to the
440 associated remains from other taxa specific to Roman-influenced Languedoc customs (Bardot-Cambot
441 and Forest, 2014; Forest, 2019; Forest, 2020 for Mureau, 2020). Measurements from this group are
442 discriminated from the other *O. edulis* groups of known origins (all from the Atlantic Ocean/English
443 Channel coastlines) and these groups are relatively close to one another. We note that the Oe_X1_A
444 and Oe_X2_A group distributions are partially overlapping (**Figure 4d**). It seems that the shells from
445 these groups of unknown origin, and found at the Antiquity Cybèle site (Lyons, over 200 km away
446 from the nearest shore), share part of their fingerprint, which could imply that all these specimens
447 lived in the same geographic region, yet not the exact same locality. Therefore, although geochemistry
448 confirms that the Cybèle groups initially determined by morphometric parameters (Bardot-Cambot,
449 2013) do exist, our data tend to discard the hypothesis that one group originated from the
450 Mediterranean Sea and the other from the Atlantic Ocean. Although additional sites from both Atlantic
451 and Mediterranean shorelines would be required to affirm this, it seems here that populations from
452 these groups lived a short distance away from each other, and the fingerprint of the Oe_X1_A group
453 seems to correspond to that of La Malène specimens (Oe_Mal_A). If true, additional specimens in
454 other localities on the Mediterranean shoreline should be analysed to identify their locality of origin,
455 but at the moment, we were not able to collect wild modern specimens.

456 **4.4. Quality of the discrimination method**

457 As our dataset is constituted of 14 elements per measurement, attempts were made to reduce
458 this number for ease of analytical and data processing work. Some elements were found to be of
459 increased importance compared to others to adequately separate measurements from different groups
460 using t-SNE. By successive removal of one element from the dataset, Pb, Ba and U are the most
461 effective at successfully discriminating *O. edulis* groups from the Mediterranean Sea and the Atlantic
462 Ocean (**Supplementary Information 7**). Rare Earth Elements (La, Ce, Pr, Nd, Sm), as found by
463 Mouchi et al. (2020a), were most useful for discriminating *C. gigas* groups. All other elements were
464 found to contribute equally to discriminating specific localities. In the end, the removal of any of the
465 measured elements systematically reduces the quality of the discriminating method.

466 Cross-validation of the clusters was attempted on *O. edulis* measurements (without the groups
467 of unknown origin, *i.e.* Oe_X1_A and Oe_X2_A) using discriminant analysis. We obtained a cross-
468 validated classification error of 24.3% (out of 210 measurements). However, when we removed all
469 measurements from the common cluster (putatively corresponding to the open marine fingerprint,
470 including all measurements from the Oe_BdV_M group) from the comparative dataset, we obtained a
471 cross-validated classification error of 0.8% (out of 123 measurements from 7 groups). Becker et al.
472 (2005) were able to retrieve an open marine origin from San Diego County mussel shell composition
473 with a 5% error (out of 41 measurements), which corresponded to misclassification to open bays.
474 However, although these specimens had been collected from six open marine localities along the
475 Pacific Ocean coastline of San Diego, the correct identification of the site had a 44 % error.
476 Misclassification of specimens from two open bays (between both bays and all open marine localities
477 as a whole) presented errors of 33 and 62 % (out of 6 and 8 measurements, respectively) due to a
478 misclassification of measurements to open marine environments. These results indicated that the open
479 marine fingerprint from the mussel shell composition is similar along 50 km of coastline (range of the
480 collection sites of the study), and that elemental fingerprinting of specimens from intertidal localities
481 in bays present some similarities to the regional open marine fingerprint. Our observations concur with
482 these conclusions, albeit with additional precision.

483

484 5. CONCLUSION

485 Previous attempts to discover the geographical origin of archaeological oyster shells based on
486 geochemistry presented various degrees of success due to the use of isotopic ratios that are strongly
487 influenced by local environmental conditions, which can be similar over extremely remote areas. In
488 this study, elemental fingerprinting of oyster shells from 15 different groups was used, highlighting
489 several points. First, different elemental incorporation behaviours prevent the direct comparison of
490 different species. Second, cluster analysis from the t-SNE method suggests that a regional fingerprint
491 seems to exist and to be distinguishable from large water bodies (seas and oceans). Third, in
492 environments with restricted influence of oceanic water, a more precise fingerprint is identified and
493 the locality (at the watershed scale) can be found. In addition, as previous studies reported, none of the
494 elements is able to differentiate between the origins of various groups on its own. Last but not least,
495 this technique was successful to identify the provenance of oyster shells of known and previously
496 unknown origin from archaeological sites. Therefore, this technique appears adequate and promising
497 to pinpoint the provenance of oyster shells. It remains necessary, however, to have the elemental
498 fingerprint of a multitude of coastal sites as a database, so that the fingerprint of unknown specimens
499 can be recognized.

500

501 6. ACKNOWLEDGEMENTS

502 This work was carried out by the support of the TracOstrea project, funded by the
503 Collaborative Research Project “*Les Marais Charentais au Moyen-Âge et à l’époque moderne*” and
504 the University of Rennes 1. The authors would like to thank Frédéric Delbès and Mikaël Guiavarch for
505 the work they performed on the preparation of the thin sections. We thank Michel Ropert from the
506 marine station of Port-en-Bessin (IFREMER), Philippe Geairon from the marine station of La
507 Tremblade (IFREMER) and Danièle Maurer from the marine station of Arcachon (IFREMER) for
508 their precious help in the breeding of oysters at Baie des Veys, Marennes-Oléron and Tès localities,

509 respectively. The authors would like to acknowledge three anonymous reviewers for their proposed
510 improvements of the manuscript and Karin Verrecchia for editing the English.

511

512 7. Data availability

513 The data used in this study have been deposited in the Zenodo data repository
514 (<http://doi.org/10.5281/zenodo.4681223>; Mouchi et al., 2021).

515

516 Declarations of interest: none.

517

518 REFERENCES

519 André, J., 1981. L'alimentation et la cuisine à Rome. *Les Belles Lettres*, Paris, 264 p.

520 Andrews, A.C., 1948. Oysters as a food in Greece and Rome. *The Classical Journal*, XLIII,
521 299-303.

522 Andrisoa, A., Lartaud, F., Rodella, V., Neveu, I., Stieglitz, T.C., 2019. Enhanced growth rates
523 of the Mediterranean mussel in a coastal lagoon driven by groundwater inflow. *Frontiers in Marine*
524 *Science*, 6, 753. doi: <https://doi.org/10.3389/fmars.2019.00753>.

525 Apolinarska, K., Kurzawska, A., 2020. Can stable isotopes of carbon and oxygen be used to
526 determine the origin of freshwater shells used in Neolithic ornaments from Central Europe?
527 *Archaeological and Anthropological Sciences*, 12, 15. doi: [https://doi.org/10.1007/s12520-019-00978-](https://doi.org/10.1007/s12520-019-00978-2)
528 [2](https://doi.org/10.1007/s12520-019-00978-2).

529 Auffret, G., 1981. Dynamique sédimentaire de la marge continentale celtique. *Ph.D. thesis*,
530 Université de Bordeaux I.

531 Bajnóczi, B., Schöll-Barna, G., Kalicz, N., Siklósi, Z., Hourmouziadis, G.H., Ifantidis, F.,
532 Kyparissi-Apostolika, A., Pappa, M., Veropoulidou, R., Ziota, C., 2013. Tracing the source of Late

533 Neolithic *Spondylus* shell ornaments by stable isotope geochemistry and cathodoluminescence
534 microscopy. *Journal of Archaeological Science*, 40, 874-882. doi: 10.1016/j.jas.2012.09.022.

535 Bambier, A., Capdeville, J.-P., Cariou, E., Floc'h, J.-P., Gabilly, J., Hantzpergue, P., 1982.
536 Notice explicative, Carte géol. France (1/50 000), feuille La Rochefoucauld (686). Orléans: BRGM,
537 30 p, Carte géologique par A. Bambier et al., 1982.

538 Bardot-Cambot, A., 2013. Les coquillages marins en Gaule romaine. Approche socio-
539 économique et socio-culturelle. *BAR International Series*, 2481, Archaeopress, Oxford, 270 p.

540 Bardot-Cambot, A., 2014. Consommer dans les campagnes de la Gaule Romaine. *Revue du*
541 *Nord*, 21, Hors-série, Collection Art et Archéologie, 109-123.

542 Bardot-Cambot, A. Forest, V., 2014. Une histoire languedocienne des coquillages marins
543 consommés, du Mésolithique à nos jours. *In*: Costamagno S. (Ed.) Histoire de l'alimentation humaine
544 : entre choix et contraintes. *Actes du 138^e congrès national des sociétés historiques et scientifiques*
545 (Rennes, 2013). Actes des congrès nationaux des sociétés historiques et scientifiques. Édition
546 électronique, p. 88-104.

547 Bayne, B.L., Ahrens, M., Allen, S.K., Anglès D'auriac, M., Backeljau, T., Beninger, P., Bohn,
548 R., Boudry, P., Davis, J., Green, T., Guo, X., Hedgecock, D., Ibarra, A., Kingsley-Smith, P., Krause,
549 M., Langdon, C., Lapègue, S., Li, C., Manahan, D., Mann, R., Perez-Paralle, L., Powell, E.N.,
550 Rawson, P.D., Speiser, D., Sanchez, J.-L., Shumway, S., Wang, H., 2017. The proposed dropping of
551 the genus *Crassostrea* for all Pacific cupped oysters and its replacement by a new genus *Magallana*: A
552 dissenting view. *Journal of Shellfish Research*, 36, 545-547. doi: 10.2983/035.036.0301.

553 Becker, B.J., Fodrie, F.J., McMillan, P.A., Levin, L.A., 2005. Spatial and temporal variation in
554 trace elemental fingerprints of mytilid mussel shells: A precursor to invertebrate larval tracking.
555 *Limnology and Oceanography*, 50, 48-61.

556 Bennion, M., Morrison, L., Brophy, D., Carlsson, J., Cortiñas Abrahantes, J., Graham, C.T.,
557 2019. Trace element fingerprinting of blue mussel (*Mytilus edulis*) shells and soft tissues successfully
558 reveals harvesting locations. *Science of the Total Environment*, 685, 50-58.

559 Bourgueil, B., Moreau, P., 1967. Notice explicative, Carte géol. France (1/50 000), feuille
560 Cognac (708). Orléans, BRGM, 12 p., Carte géologique par B. Bourgueil et P. Moreau.

561 Bourgueil, B., Moreau, P., 1970. Notice explicative, Carte géol. France (1/50 000), feuille
562 Angoulême (709). Orléans, BRGM, 20 p., Carte géologique par B. Bourgueil et P. Moreau.

563 Bourgueil, B., Moreau, P., Vouve, J., 1968. Notice explicative, Carte géol. France (1/50 000),
564 feuille Saintes (683). Orléans: BRGM, 19 p, Carte géologique par B. Bourgueil et al., 1968.

565 Bourgueil, B., Moreau, P., Gabet, C., L'Homer, A., Vouve, J., 1972. Notice explicative, Carte
566 géol. France (1/50 000), feuille Rochefort (658). Orléans: BRGM, 30 p, Carte géologique par B.
567 Bourgueil et al., 1972.

568 Campbell, G., 2010. Oysters ancient and modern: potential shape variation with habitat in flat
569 oysters (*Ostrea edulis* L.), and its possible use in archaeology, *Munibe*, Sup. 31, 176-187.

570 Carson, H.S., 2010. Population connectivity of the Olympia oyster in Southern California.
571 *Limnology and Oceanography*, 55, 134-148.

572 Champagne, A., Aoustin, D., Dupont, C., 2012. La citadelle de Brouage et la dynamique
573 paléoenvironnementale du marais charentais : l'apport de la malacologie et de la palynologie. *Bilan*
574 *Scientifique Régional 2011 de Poitou-Charentes, Service Régional de l'Archéologie*. Poitiers, 294-303.

575 Chaufourier, G., Busson, D., Dupont, C., 2015. Provenance des huîtres consommées à Lutèce
576 à la fin de la période Augustéenne. *Revue Archéologique d'Île-de-France*, 7-8, 217-229.

577 Chen, W.W. Deo, R.S., 2004. Power transformations to induce normality and their
578 applications. *Journal of the Royal Statistical Society Series B*, 66, 117-130.

579 Craig, H. 1965. The measurement of oxygen isotope palaeotemperatures. *In*: Tongiorni, E (ed.),
580 Stable isotopes in oceanographic studies and palaeotemperatures, 161–182. Pisa: Consiglio Nazionale
581 delle Ricerche Laboratorio di Geologia Nucleare.

582 Dechambenoy, C.L., Pontier, F., Sirou, F., Vouvé, J., 1977. Apport de la thermographie
583 infrarouge aéroportée à la connaissance de la dynamique superficielle des estuaires (système Charente-
584 Seudre-Anse de l'Aiguillon). *Comptes Rendus de l'Académie des Sciences de Paris*, 284, 1269-1272.

585 Dubreuilh, J., Karnay, G., Bouchet, J.-M., Le Nindre, Y.-M., 1992. Notice explicative, Carte
586 géol. France (1/50 000), feuille Arcachon (825). Orléans, BRGM, 53 p., Carte géologique par J.
587 Dubreuilh, J.-M. Bouchet.

588 Dupont, C., 2016. Could occupation duration be related to the diversity of faunal remains in
589 Mesolithic shell middens along the European Atlantic seaboard? *Quaternary International*, 407, 145-
590 153. doi : 10.1016/j.quaint.2016.01.039.

591 Durham, S.R., Gillikin, D.P., Goodwin, D.H., Dietl, G.P., 2017. Rapid determination of oyster
592 lifespans and growth rates using LA-ICP-MS line scans of shell Mg/Ca ratios. *Palaeogeography*,
593 *Palaeoclimatology, Palaeoecology*, 485, 201-209. Doi: 10.1016/j.palaeo.2017.06.013.

594 Eerkens, J.W., Herbert, G.S., Rosenthal, J.S., Spero, H.J., 2005. Provenance analysis of
595 *Olivella biplicata* shell beads from the California and Oregon Coast by stable isotope fingerprinting.
596 *Journal of Archaeological Science*, 32, 1501-1514.

597 Eerkens, J.W., Rosenthal, J.S., Stevens, N.E., Cannon, A., Brown, E.L., Spero, H.J., 2010.
598 Stable isotope provenance analysis of *Olivella* shell beads from the Los Angeles Basin and San
599 Nicolas Island. *Journal of Island & Coastal Archaeology*, 5, 105-119. Doi:
600 10.1080/15564890902955327.

601 Fodrie, F.J., Becker, B.J., Levin, L.A., Gruenthal, K., McMillan, P.A., 2011. Connectivity
602 clues from short-term variability in settlement and geochemical tags of mytilid mussels. *Journal of*
603 *Sea Research*, 65, 141-151.

604 Forest, V., 2019. Les paysans consommateurs et les vestiges fauniques archéologiques : une
605 fausse évidence. In: G. Ferrand, J. Petrowiste (Eds.) Le nécessaire et le superflu. Le paysan
606 consommateur. *Actes des XXXVI^e Journées internationales d'histoire de l'Abbaye de Flaran*, October
607 17th-18th 2014, Presses Universitaires du Midi, Toulouse, pp.69-78.

608 Forest, V., 2020. Étude archéozoologique préliminaire : conchyliologie. La Malène – Les
609 Piboulèdes (Lozère) (périodes antique et médiévale). Rapport inédit.

610 Gruet, Y., Prigent, D., 1986a. Etude de deux prélèvements d'huîtres d'époque gallo-romaine
611 provenant d'Alet (Saint-Malo). *Les Dossiers du CeRAA*, 14, 123-129.

612 Gruet, Y., Prigent, D., 1986b. Les buttes de Saint-Michel-en-l'Herm (Vendée) : caractères de
613 la population d'huîtres (*Ostrea edulis* Linné) et de sa faune associée. *Haliotis*, 15, 3-16.

614 Hantzpergue, P., Bonnin, J., Cariou, E., Gomez de Soto, J., Moreau, P., 1984. Notice
615 explicative, Carte géol. France (1/50 000), feuille Mansle (685). Orléans: BRGM, 24 p, Carte
616 géologique par P. Hantzpergue et al., 1984.

617 Herz, N., Waelkens, M., 1988. Classical marble: Geochemistry, Technology, Trade. Springer-
618 Science + Business Media, SV, 464 p.

619 Huyghe, D., de Rafelis, M., Ropert, M., Mouchi, V., Emmanuel, L., Renard, M., Lartaud, F.,
620 2019. New insights into oyster high-resolution hinge growth patterns. *Marine Biology*, 166, 48.

621 Huyghe, D., Emmanuel, L., de Rafelis, M., Renard, M., Ropert, M., Labourdette, N., Lartaud,
622 F., 2020. Oxygen isotope disequilibrium in the juvenile portion of oyster shells biases seawater
623 temperature reconstructions. *Estuarine, Coastal and Shelf Science*, 240, 106777.

624 Jackson, S.E., 2008. LAMTRACE data reduction software for LA-ICP-MS. In: Laser ablation
625 ICP-MS in the Earth sciences: Current practices and outstanding issues. *The Canadian Mineralogist*,
626 40, 305-307.

627 Jochum, K.P., Nohl, U., Herwig, K., Lammel, E., Stoll, B., Hofmann, A.W., 2005. GeoReM:
628 A new Geochemical database for reference materials and isotopic standards. *Geostandards and*
629 *Geoanalytical Research*, 29, 333-338, doi 10.1111/j.1751-908X.2005.tb00904.x.

630 Kirby, M.X., Soniat, T.M., Spero, H.J., 1998. Stable isotope sclerochronology of Pleistocene
631 and recent oyster shells (*Crassostrea virginica*). *Palaios*, 13, 560–569.

632 Kuzmin, Y.V., Alekseyev, A.N., Dyakonov, V.M., Grebennikov, A.V., Glascock, M.D., 2018.
633 Determination of the source for prehistoric obsidian artifacts from the lower reaches of Kolyma River,
634 Northeastern Siberia, Russia, and its wider implications. *Quaternary International*, 476, 95-101.

635 Lartaud, F, Emmanuel, L, de Rafélis, M, Pouvreau, S, Renard, M. 2010a. Influence of food
636 supply on the $\delta^{13}\text{C}$ signature of mollusc shells: implications for palaeoenvironmental reconstitutions.
637 *Geo-Marine Letters*, 30, 23–34. Doi: <https://doi.org/10.1007/s00367-009-0148-4>.

638 Lartaud, F., de Rafélis, M., Ropert, M., Emmanuel, L., Geairon, P., Renard, M., 2010b. Mn
639 labelling of living oysters: artificial and natural cathodoluminescence analyses as a tool for age and
640 growth rate determination of *C. gigas* (Thunberg, 1793) shells. *Aquaculture*, 300 (1), 206-217, doi
641 10.1016/j.aquaculture.2009.12.018.

642 Lartaud, F., Emmanuel, L., de Rafélis, M., Ropert, M., Labourdette, N., Richardson, C.A.,
643 Renard, M., 2010c. A latitudinal gradient of seasonal temperature variation recorded in oyster shells
644 from the coastal waters of France and The Netherlands. *Facies*, 56, 13, doi 10.1007/s10347-009-0196-
645 2.

646 Lazure, P., Desmare, S., 2012. Manche – Mer du Nord – Etat physique et chimique,
647 caractéristiques physiques, courantologie. *Caractéristiques et Etat Ecologique*, 9 p.
648 https://www.ifremer.fr/sextant_doc/dcsmm/documents/Evaluation_initiale/MMN/EE/MMN_EE_06_C
649 [ourantologie.pdf](https://www.ifremer.fr/sextant_doc/dcsmm/documents/Evaluation_initiale/MMN/EE/MMN_EE_06_C).

650 Matthews, K.J., 1997. The establishment of a data base of neutron activation analyses of white
651 marble. *Archaeometry*, 39, 321-332.

652 Michelaki, K., Hughes, M.J., Hancock, R.G.V., 2013. On establishing ceramic chemical
653 groups: exploring the influence of data analysis methods and the role of the elements chosen in
654 analysis. In: R.H. Tykot (ed.) Proceedings of the 38th International Symposium on Archeometry – May
655 10th - 14th 2010, Tampa, Florida. *Open Journal of Archaeometry*, 1, e1.

656 Milano, S., Schöne, B.R., Gutiérrez-Zugasti, I., 2019. Oxygen and carbon stable isotopes of
657 *Mytilus galloprovincialis* Lamarck, 1819 shells as environmental and provenance proxies. *The*
658 *Holocene*. Doi: 10.1177/0959683619865595.

659 Monbet, Y., Bassoulet, P., 1989. Bilan des connaissances océanographiques en rade de Brest.
660 *Rapport technique*, IFREMER, CEA/IPSN, 106 p.

661 Morrison, L., Bennion, M., Gill, S., Graham, C.T., 2019. Spatio-temporal trace element
662 fingerprinting of king scallops (*Pecten maximus*) reveals harvesting period and location. *Science of the*
663 *Total Environment*, 697, 134121.

664 Mouchi, V., de Rafélis, M., Lartaud, F., Fialin, M., Verrecchia E., 2013. Chemical labelling of
665 oyster shells used for time-calibrated high resolution Mg/Ca ratios: a tool for past estimation of seasonal
666 temperature variations. *Palaeogeography Palaeoclimatology Palaeoecology*, 373, pp. 66-74.

667 Mouchi, V., Briard, J., Gaillot, S., Argant, T., Forest, V., Emmanuel, L., 2018. Reconstructing
668 environments of collection site from archaeological bivalve shells: case study from oysters (Lyon,
669 France). *Journal of Archaeological Science: Reports*, 21, 1225-1235. doi: 10.1016/j.jasrep.2017.10.025.

670 Mouchi, V., Godbillot, C., Forest, V., Ulianov, A., Lartaud, F., de Rafélis, M., Emmanuel, L.,
671 Verrecchia, E.P., 2020a. Rare earth elements in oyster shells: provenance discrimination and potential
672 vital effects. *Biogeosciences*, 17, 2205–2217. doi: <https://doi.org/10.5194/bg-17-2205-2020>.

673 Mouchi, V., Emmanuel, L., Forest, V., Rivalan, A., 2020b. Geochemistry of bivalve shells as
674 indicator of shore position of the 2nd century BC. *Open Quaternary*, 6, 4, 1-15. doi:
675 <https://doi.org/10.5334/oq.65>.

676 Mouchi, V., Godbillot, C., Dupont, C., Vella, M.-A., Forest, V., Ulianov, A., Lartaud, F., de
677 Rafélis, M., Emmanuel, L., Verrecchia, E.P., 2021. Data for the publication by Mouchi et al.
678 "Provenance study of oyster shells by LA-ICP-MS" [Data set]. Zenodo.
679 <http://doi.org/10.5281/zenodo.4681223>.

680 Mourier, J.-P., Floc'h, J.-P., Coubès, L., 1989. Notice explicative, Carte géol. France (1/50 000),
681 feuille L'Isle-Jourdain (638). Orléans: BRGM, 73 p, Carte géologique par J.-P. Mourier et al., 1989.

682 Mrozek-Wysocka, M., 2014. 5. Ancient marbles: Provenance determination by archaeometric
683 study. In: D. Michalska & M. Szcsepaniak (eds.) *Geoscience in Archaeometry. Methods and case*
684 *studies*. Bogucki Wydawnictwo Naukowe, Poznań, 195 p.

685 Mureau, C., 2020. Consommation et exploitation des ressources animales dans l'est du Massif
686 central et le Languedoc de la fin de l'Antiquité tardive au haut Moyen Âge. *Ph.D. thesis*, Université de
687 Bourgogne-Franche-Comté, Dijon.

688 Normand, E., Champagne, A., et alii, 2019. Broue (Saint-Sornin – Charente-Maritime) : un site
689 élitaire au coeur des marais charentais. *Rapport intermédiaire de fouille programmée triennale –*
690 *campagne 2019*, SRA Nouvelle-Aquitaine – site de Poitiers, 236 p.

691 Orsoni, V., Souchu, P., Sauzade, D., 2001. Caractérisation de l'état d'eutrophisation des trois
692 principaux étangs corses (Biguglia, Diana et Urbino), et proposition de renforcement de leur
693 surveillance. Rapport final. R.INT.DEL/CO 00-02. <https://archimer.ifremer.fr/doc/00074/18534>.

694 Platel, J.-P., Moreau, P., Vouvé, J., Colmont, G.R., 1977. Notice explicative, Carte géol. France
695 (1/50 000), feuille Pons (707). Orléans: BRGM, 43 p, Carte géologique par J.-P. Platel et al., 1977.

696 Platel, J.-P., Moreau, P., Vouvé, J., Debenath, A., Colmont, G.R., Gabet, C., 1978. Notice
697 explicative, Carte géol. France (1/50 000), feuille St-Agnant (682). Orléans: BRGM, 52 p, Carte
698 géologique par J.-P. Platel et al., 1978.

699 Querré, G., Cassen, S., Calligaro, T., 2015. Témoin d'échanges au Néolithique le long de la
700 façade atlantique : la parure en variscite des tombes de l'ouest de la France. In: N., Naudinot, L.,

701 Meignen, D., Binder, G., Querré (eds.) *Les systèmes de mobilité de la Préhistoire au Moyen Age. Actes*
702 *des 35^e rencontres internationales d'archéologie et d'histoire d'Antibes*, October 14th-16th 2014, 403-
703 418. Editions APDCA, Antibes.

704 Ricardo, F., Pimentel, T., Génio, L., Calado, R., 2017. Spatio-temporal variability of trace
705 elements fingerprints in cockle (*Cerastoderma edule*) shells and its relevance for tracing geographic
706 origin. *Scientific Reports*, 7, 3475. Doi: 10.1038/s41598-017-03381-w.

707 Richardson, C.A., Collis, S.A., Ekaratne, K., Dare, P., Key, D., 1993. The age determination
708 and growth rate of the European flat oyster, *Ostrea edulis*, in British waters determined from acetate
709 peels of umbo growth lines. *ICES Journal of Marine Science*, 50, 493–500.

710 Robin, A.-K., Mouralis, D., Akköprü, Gratuze, B., Kuzucuoğlu, C., Nomade, S., Pereira, A.,
711 Doğu, A.F., Erturaç, K., Khalidi, L., 2016. Identification and characterization of two new obsidian sub-
712 sources in the Nemrut volcano (Eastern Anatolia, Turkey): The Sıcaksu and Kayacık obsidian. *Journal*
713 *of Archaeological Science: Reports*, 9, 705-717.

714 Salvi, D., Mariottini, P., 2016. Molecular taxonomy in 2D: a novel ITS2 rRNA sequence
715 structure approach guides the description of the oysters' subfamily *Saccostreinae* and the genus
716 *Magallana* (Bivalvia: Ostreidae). *Zoological Journal of the Linnean Society*, 179, 263-276.
717 <https://doi.org/10.1111/zoj.12455>.

718 Schneider, M., Lepetz, S., 2007. L'exploitation, la commercialisation et la consommation des
719 huîtres à l'époque romaine en Gaule : origine géographique et source d'approvisionnement des huîtres
720 du vieil Evreux et de Chartres. *Publication des actes du colloque 'Les nourritures de la mer, de la criée*
721 *à l'assiette'*. Colloque de Tatihou organisé par la SFHM du 2 au 4 octobre 2003, p11-34.

722 Shackleton, N., Renfrew, C., 1970. Neolithic trade routes re-aligned by oxygen isotope analyses.
723 *Nature*, 228, 1062-1065.

724 Sharp, Z. 2007. Principles of stable isotope geochemistry. Upper Saddle River, NJ: Pearson
725 Prentice Hall, 360 p.

726 Somerville, L., Light, J., Allen, M.J., 2017. Marine molluscs from archaeological contexts:
727 how they can inform interpretations of former economies and environments. *In*: M.J. Allen (Ed.)
728 *Molluscs in Archaeology*, 214-237.

729 Sorte, C.J.B., Etter, R.J., Spackman, R., Boyle, E.E., Hannigan, R.E., 2013. Elemental
730 fingerprinting of mussel shells to predict population sources and redistribution potential in the Gulf of
731 Maine. *PLoS ONE*, 8, e80868.

732 Urey, H.C., Lowenstam, H.A., Epstein, S., McKinney, C.R., 1951. Measurements of
733 paleotemperatures and temperatures of the Upper Cretaceous of England, Denmark, and the
734 southeastern United States. *Bulletin of the Geological Society of America*, 62, 399-416.

735 van der Maaten, L. Hinton, G., 2008. Visualizing data using t-SNE. *Journal of Machine*
736 *Learning Research*, 9, 2579-2605.

737 Vogl, J., Paz, B., Völling, E., 2019. On the ore provenance of the Trojan silver artefacts.
738 *Archaeological and Anthropological Sciences*, 11, 3267-3277.

739 Zhao, H., Zhang, S., 2016. Effects of sediment, seawater, and season on multi-element
740 fingerprints of Manila clam (*Ruditapes philippinarum*) for authenticity identification. *Food Control*,
741 66, 62-68. Doi: 10.1016/j.foodcont.2016.01.045.